Chapter 2

Numerical Modelling of the Plasma Focus Discharge

2.1 The dynamic model of the plasma focus

The oldest method used to generate high temperature dense magnetized plasma has been based on high current pulse discharge between metal electrodes. An important electrode configuration is a system consisting of two coaxial electrodes (inner and outer electrodes) of different diameters, separated by a tubular glass or a ceramic insulator embracing the inner electrode at the beginning. After filling the chamber with a working gas (usually under a low pressure) the discharge is initiated by the application of a high-voltage pulse between two electrodes. The inner electrode (acting as the anode) is usually connected to the high voltage while the outer electrode (acting as the cathode) is connected to the ground. As the breakdown begins along the insulator surface, a current sheath develops and gives rise to an azimuthal magnetic field, which drives the current sheath towards the end of the electrodes. After reaching the electrode ends, it is subjected to a radial collapse towards the system axis. Finally it focuses into a plasma column at the tip of the inner electrode. The dynamics of a plasma focus discharge can be considered to be consisting of 4 phases (Figure 2.1), which are:

1) The breakdown and current-sheath formation phase
2) The axial acceleration phase
3) The radial pinch compression phase
4) The dense plasma focus phase

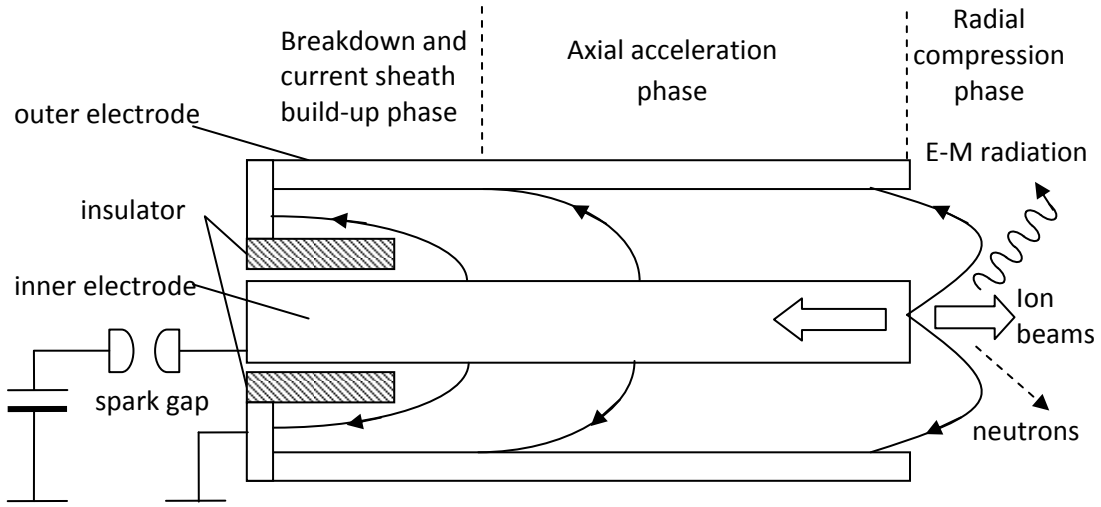

Figure 2.1: Schematic of the different phases of the discharge in a plasma focus device.

2.1.1 The breakdown and current-sheath formation phase

In a Mather type plasma focus, the two electrodes are separated by a cylindrical insulator sleeve at the back wall of the discharge tube. A plasma focus discharge is initiated by the application of a high-voltage pulse between two electrodes where consequently a dense plasma layer (a current sheath) is formed along the cylindrical insulator surface. This current sheath will be pushed away from the insulator surface by the $\bar{J} \times \bar{B}$ force (where $\bar{J}$ is the current density and $\bar{B}$ is the self-magnetic field) until it becomes perpendicular to the electrodes and ready to move in the axial direction (z-direction) as shown in Figure 2.2.

The plasma layer in the axial acceleration phase can be simplified as a flat annular conductive sheath connecting the anode to the cathode in modelling. In a real discharge, however, the magnetic pressure is greatest next to the anode due to the radial distribution of the magnetic field in the space between the electrodes. Therefore, the

plasma moves faster next to the anode, and the layer moves in a canted fashion with the part next to the anode leading.

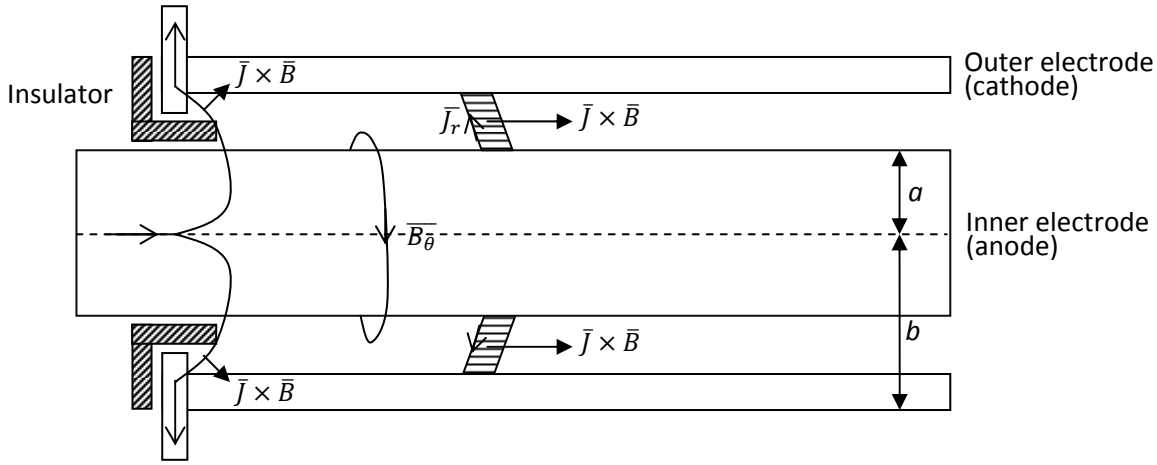

Figure 2.2: The schematic diagram of the formation and lift-off of the current sheath.

2.1.2 The axial acceleration phase

During the axial acceleration phase (which is very similar to the electromagnetic shock tube), the current sheath is driven by the electromagnetic force and accelerates down the electrodes. The current sheath acts like a piston and sweeps away all ionized gas molecules that it encounters with.

The azimuthal magnetic field $\overline{B_\theta}$ is generated by the coaxial discharge current and is given by

$$\overline{B_\theta} = \frac{\mu_0 I}{2\pi r}$$

where μ_0 is the permeability of free space, I is the discharge current and r is the radial position. As this magnetic field only presents behind the current sheath therefore the magnetic field ahead of the current sheath is zero. Since $\overline{B_\theta}$ is dependent on the radial

position *r* then the magnetic field is stronger at the surface of the inner electrode and becomes weaker towards the inner surface of the outer electrode. The effect of the difference in the magnetic field strength between the inner electrode and outer electrode is the slanting structure of the electromagnetic piston as shown in Figure 2.2. Nevertheless, the dynamic of the current sheath in this axial acceleration phase can be sufficiently accurate modelled by simply assuming the current sheath to be vertical to the electrodes from the surface of the inner electrode to the outer electrode. In this case, the $\bar{J} \times \bar{B}$ force (electromagnetic piston) acting in the z-direction can be expressed as

$$\int_a^b \frac{{B_\theta}^2}{2\mu_0} 2\pi r dr$$

where *a* is the radius of the inner electrode and *b* is the radius of the outer electrode. This electromagnetic force drives the electromagnetic piston to a supersonic speed so that a shock heated layer of plasma is formed.

The dynamics of the electromagnetic piston can be modelled by using the geometry of the plasma focus as shown in Figure 2.2. The current sheet is assumed to start from zero velocity at the position when it first becomes vertical to the electrodes, hence the effective length of the electrodes (z_0) should be measured from the edge of the cylindrical insulator.

Based on the observation of a 58-160 J plasma focus device operated in repetitive mode using fast pseudospark switch [Hassan, 2006], the estimated duration of initial breakdown to acceleration phase is about 250-350 ns. The expected time estimate for the axial phase is based on typical axial speed of 3 – 7 cm/μs for most of the Mather-

type plasma focus devices. Whilst, according to the optical imaging data reported, the duration of the initial breakdown phase until the axial acceleration phase takes about 380 ns – 400 ns and the subsequent radial compression phase lasts for the next 200 ns. The average axial current speed was estimated to be approximately 3.5 cm/μs.

2.1.3 The radial pinch compression phase

After the breakdown at the base of the plasma gun along the insulator surface, a current sheath is developed and gives rise to an azimuthal magnetic field, which the self generated Lorentz force drives the current sheath towards the end of the electrodes. The current sheath sweeps up the ionized gas and leaves behind a vacuum region. This current sheath first undergoes an axial acceleration and upon reaching the end of the electrodes, it is subjected to a radial collapse towards the system axis. Finally it focuses into a plasma column at the tip of the inner electrode. The sudden collapse of the current sheath towards the axis at the center electrode end is most likely caused by the rapid conversion of stored magnetic energy into radial sheath motion forming a super dense pinch. The radial speed, $\overline{v_r}$ of the current sheath first measured by Mather is about $3.5 \times 10^7 \text{cm s}^{-1}$ [Mather, 1965].

When focusing occurs, a rapid compression of plasma takes place. The strong electro-mechanical action draws energy from the magnetic field, pumping the energy into the compressed plasma. This mechanism results in a distinctive current dip and a voltage spike on the discharge current and voltage oscillogram. Large amplitude of the

spike in the voltage signal and the dip in the current signal are indications of strong focusing [Nisar, 1993].

When the current sheath reaches the end of the inner electrode, the motion of the current sheath shall be modelled in 2-dimensions. The current sheath will continue to move in the z-direction thus it may extend out of the inner electrode. While its length is increasing the plasma column is being pinch radially at the same time. In other words, the radial pinch compression phase is similar to an elongating Z-pinch plasma. At the beginning, the height of the plasma column is practically equal to zero and its radius is that of the anode of the apparatus. As time goes on, it elongates and contracts simultaneously, yielding at the end the formation of a dense cylindrical pinch of about 1 mm diameter, as depicted in Figure 2.3.

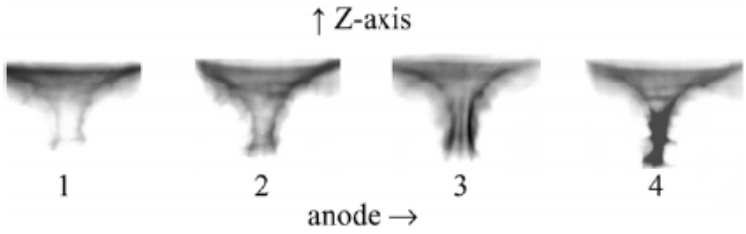

Figure 2.3: The streak photographs showing the radial compression phase in four frames taken by an optical image camera with 1 ns time resolution [Gribkov, 2007].

2.2 Modelling of the plasma focus dynamics

2.2.1 The axial acceleration phase computational model – (The Snow-plow model)

The second phase of a plasma focus discharge, which is the axial acceleration of the current sheath, can be computed using the snow-plow model. This model was originally developed by Marshal Rosenbluth in the 50s. In a simplified snow-plow theory, the current sheath is assumed to be infinitely thin, thus the magnetic piston edge,

the current sheath and the shock form the same interface. The rate of change of momentum of the current sheath in a one dimensional snow-plow model can be written as

$$\frac{d(mv)}{dt} = \frac{d}{dt}\left\{[\rho_0\pi(b^2 - a^2)z]f_m\frac{dz}{dt}\right\}$$

$$= \rho_0\pi(c^2 - 1)a^2 f_m\frac{d}{dt}\left(z\frac{dz}{dt}\right)$$

Where z is the axial position, ρ_0 is the ambient gas density, b is the radius of the outer electrode, a is the radius of the inner electrode (as shown in Figure 2.2), z is the distance of the current sheath from the insulator surface, c is $\left({}^{b}/_{a}\right)$ and f_m is the fraction of mass swept down the tube in the z-direction.

The snow plow model has been used extensively to describe the axial phase of the plasma focus discharge [Lee, 1983].As Barbaglia et al. (2010) suggested that the actual current sheath propagating in the plasma focus tube which is not plane but canted, that its kinematics can be resolved into both axial and radial directions. It is appropriate to adjust the equivalent swept mass to the experimental observations, which experimental observations is smaller than the total mass calculated using the filling gas density. Thus f_m is introduced in the equation of motion of the current sheath as to reduce the percentage of mass swept up by the current sheath.

The magnetic force (Lorentz force) acting on the current sheath is

$$F = \int_a^b \left[\left(\frac{\mu_0 I f_c}{2\pi r}\right)^2 / (2\mu_0)\right] 2\pi r dr = \frac{\mu_0 {f_c}^2}{4\pi} ln(c) I^2$$

where μ_0 is the permeability of free space ($4\pi\times10^{-7}$ Hm^{-1}), I is the coaxial discharge current, r is the radial position of the azimuthal magnetic field B_θ and f_c is the fraction of current flowing in the piston. Considering that the Lorentz force ($J\times B$) which acts on the current sheath equals the rate of change in the linear momentum of the current sheath, thus, the equation of motion for the piston (current sheath) can be written as

$$\rho_0\pi(c^2-1)a^2 f_m\left[\frac{d}{dt}\left(z\frac{dz}{dt}\right)\right]=\frac{\mu_0 {f_c}^2}{4\pi}ln(c)I^2$$

Thus, the acceleration of the current sheath is expressed as

$$\therefore \frac{d^2z}{dt^2}=\frac{\left[\frac{{f_c}^2}{f_m}\frac{\mu_0(lnc)}{4\pi^2\rho_0(c^2-1)}\left(\frac{I}{a}\right)^2-\left(\frac{dz}{dt}\right)^2\right]}{z} \ldots\ldots (2.1)$$

The effect of the dynamics of the current sheath on the discharge current is taken into consideration by solving the equation of motion and the coupled circuit equation simultaneously. The coupled circuit equation is written based on the equivalent circuit of the capacitor discharge system (Figure 2.4) where the plasma is represented by L_p. The plasma focus discharge system is assumed to be inductive. By writing

$$\frac{d}{dt}\left[(L_0+L_p)I\right]\gg I(R_0+R_p)$$

The circuit equation can be simplified as

$$\frac{d}{dt}\left[(L_0+L_pf_c)I\right]=V_0-\frac{\int_0^t Idt}{C_0}$$

$$(L_0+L_pf_c)\frac{dI}{dt}+If_c\frac{dL}{dt}=V_0-\int\frac{Idt}{C_0}$$

By substituting the plasma inductance as

$$L_p = \frac{\mu_0 z}{2\pi} ln(c) \quad \text{and} \quad \frac{dL_p}{dt} = \frac{\mu_0}{2\pi} ln(c)\ \frac{dz}{dt}$$

The rate of change of current is obtained as

$$\frac{dI}{dt} = \frac{V_0 - \frac{\int Idt}{C_0} - \frac{\mu_0}{2\pi} ln(c)\ I f_c \frac{dz}{dt}}{L_0 + \frac{\mu_0 f_c}{2\pi} ln(c)\ z} \ldots\ldots (2.2)$$

This equation will be solved simultaneously with the equation of motion.

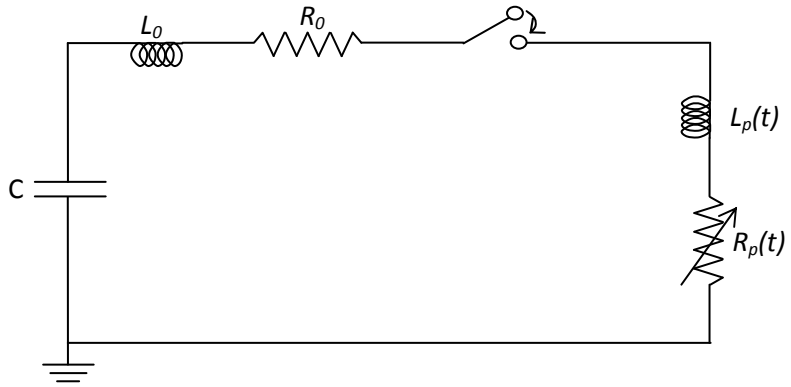

Figure 2.4: The schematic circuit of the capacitor discharge system.

As for the convenience of solving these equations, the following normalized parameters are chosen:

$$\zeta = \frac{z}{z_0}, \quad \tau = \frac{t}{t_0}, \quad \imath = \frac{I}{I_0}$$

Where z_0 : effective length of the electrodes

$I_0 = V_0\sqrt{C/L_0}$: peak current of the short circuited capacitor bank

$t_0 = \sqrt{L_0 C}$: discharge characteristic time

The normalization of Equation (2.1) is

$$\frac{z_0}{{t_0}^2}\frac{d^2\zeta}{d\tau^2} = \frac{\left[\frac{{f_c}^2}{f_m}\frac{\mu ln(c)}{4\pi^2\rho_0(c^2-1)}\left(\frac{I_0}{a}\right)^2 \iota^2 - \frac{{z_0}^2}{{t_0}^2}\left(\frac{d\zeta}{d\tau}\right)^2\right]}{z_0\zeta}$$

$$\frac{d^2\zeta}{d\tau^2} = \frac{\frac{{f_c}^2}{f_m}\frac{\mu ln(c)}{4\pi^2\rho_0(c^2-1)}\left(\frac{I_0}{a}\right)^2 \frac{{t_0}^2}{{z_0}^2}\iota^2 - \left(\frac{d\zeta}{d\tau}\right)^2}{\xi}$$

$$\frac{d^2\zeta}{d\tau^2} = \frac{\alpha^2\iota^2 - \left(\frac{d\zeta}{d\tau}\right)^2}{\zeta} \dots\dots (2.3)$$

Where

$$\alpha^2 = \left(\frac{t_0}{t_a}\right)^2 \quad \text{and} \quad {t_a}^2 = \frac{f_m}{{f_c}^2}\frac{4\pi^2\rho_0{z_0}^2(c^2-1)a^2}{\mu_0{I_0}^2 ln(c)}$$

Which $\alpha = \left(\frac{t_0}{t_a}\right)$ is the ratio of the electrical discharge time to characteristic axial transit time.

The normalization of circuit equation (2.2) is

$$\frac{I_0}{t_0}\frac{d\iota}{d\tau} = \frac{V_0 - \frac{I_0 t_0}{C_0}\int \iota d\tau - I_0\, \iota f_c \frac{\mu_0}{2\pi} ln(c)\left(\frac{z_0}{t_0}\right)\frac{d\zeta}{d\tau}}{L_0 + \frac{f_c\mu_0}{2\pi} ln(c) z_0\zeta}$$

Substitute

$$I_0 = \frac{V_0}{\sqrt{\frac{L_0}{C_0}}}, \quad t_0 = \sqrt{L_0 C_0}$$

$$\frac{d\iota}{d\tau} = \frac{1 - \int \iota d\tau - \left[f_c\left(\frac{\mu_0}{2\pi}\right) ln(c)\left(\frac{Z_0}{L_0}\right)\right]\iota\frac{d\zeta}{d\tau}}{\left[1 + \left(\frac{f_c\mu_0}{2\pi} ln(c) z_0\right)\frac{\zeta}{L_0}\right]}$$

$$\frac{d\iota}{d\tau} = \frac{1 - \int \iota d\tau - f_c \frac{\mu_0 z_0}{2\pi L_0} ln(c) \iota \frac{d\zeta}{d\tau}}{1 + f_c \frac{\mu_0 z_0}{2\pi L_0} ln(c) \zeta}$$

Thus,

$$\frac{d\iota}{d\tau} = \frac{1 - \int \iota d\tau - \iota\beta \frac{d\zeta}{d\tau}}{1 + \beta\zeta} \dots\dots (2.4)$$

Which

$$L_a = \frac{f_c \mu_0}{2\pi} ln(c) z_0$$

is the inductance of the axial phase when the current sheath reaches the end of the tube, $z = z_0$.

Therefore, the second scaling parameter

$$\beta = \frac{L_a}{L_0}$$

is the ratio of load to source inductance.

The two normalized equations (Equation 2.3 and Equation 2.4) can be integrated by taking the following initial conditions:

$$\tau = 0, \quad \zeta = 0, \quad \frac{d\zeta}{d\tau} = 0, \quad \frac{d^2\zeta}{d\tau^2} \xrightarrow{\tau \to 0} \frac{\alpha}{\sqrt{2}}, \ \iota = 0, \quad \int \iota d\tau = 0, \ \frac{d\iota}{d\tau} = 1$$

Setting time increment, $\Delta\tau = 0.001$

Next step values are computed using the following approximation:

$$\tau_{n+1} = \tau_n + \Delta\tau$$

$$\zeta_{n+1} = \zeta_n + \left(\frac{d\zeta}{d\tau}\right)_n \Delta\tau + \frac{1}{2}\left(\frac{d^2\zeta}{d\tau^2}\right)\Delta\tau^2$$

$$\left(\frac{d\zeta}{d\tau}\right)_{n+1} = \left(\frac{d\zeta}{d\tau}\right)_n + \left(\frac{d^2\zeta}{d\tau^2}\right)_n \Delta\tau$$

$$\frac{d^2\zeta}{d\tau^2} = \frac{\left[\alpha^2\iota^2 - \left(\frac{d\zeta}{d\tau}\right)^2\right]}{\zeta}$$

$$\iota_{n+1} = \iota_n + \left(\frac{d\iota}{d\tau}\right)_n \Delta\tau$$

$$\int \iota d\tau_{n+1} = \int \iota d\tau_n + \iota_n \Delta\tau$$

$$\frac{d\iota}{d\tau} = \frac{\left[1 - \int \iota d\tau - \beta\iota\frac{d\zeta}{d\tau}\right]}{1 + \beta\zeta}$$

The computation stops when $\zeta = 1$ $(z = z_0)$

2.2.2 The radial pinch compression phase (Slug model)

As per the simulation of the axial acceleration made using the snow-plow model, the current sheath is assumed to be infinitely thin. When the current sheath reaches the end of the electrode, this will lead to all current flowing at zero radius, which will result in infinite inductance and density. Thus, a slug model is employed instead of the snow plow model to describe the radial compression phase. This will allow us to

quantitatively measure the change in impedance during the compression and pinch formation. In this model, the magnetic pressure drives a shock wave ahead of it and creates a space for the current sheath to move into (Figure 2.5).

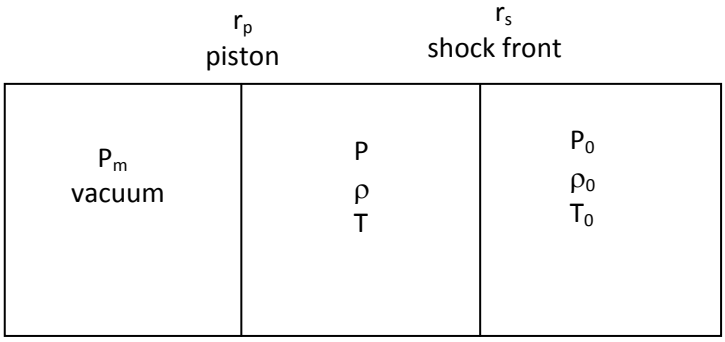

Figure 2.5: The motion of the shock front and the piston (current sheath).

The motion of the shock front can be explained using the shock wave theory. When the piston propagates through the ambient gas (which density is ρ_0) with shock speed, v_s, the pressure of the shock heated gas will rise abruptly to value P.

The shock pressure, P, can be written as

$$P = \frac{2}{\gamma + 1}\rho_0 {v_s}^2$$

Assuming that this pressure, P, is uniform from the current sheath to the shock front, thus,

$$P = P_m = \frac{\left(\mu I f_c / 2\pi r_p\right)^2}{2\mu}$$

and

$${v_s}^2 = \frac{\mu (I f_c)^2}{8\pi^2 {r_p}^2} \times \frac{\gamma + 1}{2\rho_0 f_{mr}}$$

Where I is the circuit current, γ is the specific heat ratio of the plasma, f_c is the fraction of current flowing in the current sheath (taken as the same value of f_c obtained in the

axial phase), f_{mr} is the fraction of mass swept into the radial slug which is different from f_m of the axial phase.

Hence, the radial speed of the shock front is

$$\frac{dr_s}{dt} = -\left[\frac{\mu(\gamma+1)}{\rho_0}\right]^{\frac{1}{2}} \frac{f_c}{\sqrt{f_{mr}}} \frac{I}{4\pi r_p} \qquad \ldots\ldots (2.5)$$

After the current sheath has reached the end of the electrode, it is still moving in the axial direction (at the same time it is moving in the radial direction as mentioned above). This causes the plasma column to elongate in the axial direction. The pressure driving the axial shock is the same as the pressure driving the inward radial shock. Therefore, the axial shock speed is the same as the radial speed. However, the current sheath should be moving at a slower speed than the shock, which the speed can be approximated by a factor of $\frac{2}{(\gamma+1)}$ (from shock wave theory), that is

$$\frac{dz_f}{dt} = -\left(\frac{2}{\gamma+1}\right)\frac{dr_s}{dt} \qquad \ldots\ldots (2.6)$$

Using an adiabatic relationship to relate the radial shock front motion, dr_s with the driving current, I, the plasma slug pressure, P, and plasma slug volume, V, we obtain

$$PV^{\gamma} = constant$$

or

$$\frac{\gamma dV}{V} + \frac{dP}{P} = 0$$

where slug pressure, P is proportional to v_s^2 ($P \sim v_s^2$), therefore

$$\frac{dP}{P} = \frac{2dv_s}{v_s}$$

but

$$v_s \sim \frac{I}{r_p}$$

so

$$\frac{dP}{P} = 2\left(\frac{dI}{I} - \frac{dr_p}{r_p}\right)$$

The slug volume, $V = \pi\left({r_p}^2 - {r_s}^2\right)z_f$

The increase in volume is given as

$$dV = 2\pi\left(r_p dr_p - \frac{2}{\gamma+1} r_s dr_s\right)z_f + \pi\left({r_p}^2 - {r_s}^2\right)dz_f$$

Note that a factor of $\frac{2}{\gamma+1}$ is added in the above expression is because the swept up gas is compressed by a ratio of $\frac{(\gamma+1)}{(\gamma-1)}$ which will contribute to the increase in slug volume, *V*.

Thus, we can write

$$\frac{\gamma dV}{V} = \frac{2\gamma\left(r_p dr_p - \frac{2}{\gamma+1} r_s dr_s\right)z_f + \gamma\left({r_p}^2 - {r_s}^2\right)dz_f}{z_f\left({r_p}^2 - {r_s}^2\right)}$$

By adding together $\frac{dP}{P}$ and $\frac{\gamma dV}{V}$, we have

$$\frac{2\gamma\left(r_p dr_p - \frac{2}{\gamma+1} r_s dr_s\right)z_f + \gamma\left({r_p}^2 - {r_s}^2\right)dz_f}{z_f\left({r_p}^2 - {r_s}^2\right)} + 2\frac{dI}{I} - 2\frac{dr_p}{r_p} = 0$$

Rearranging, we have

$$\frac{dr_p}{dt} = \frac{\frac{2}{\gamma+1}\frac{r_s}{r_p}\frac{dr_s}{dt} - \frac{r_p}{\gamma I}\left(1-\frac{{r_s}^2}{{r_p}^2}\right)\frac{dI}{dt} - \frac{1}{(\gamma+1)}\frac{r_p}{z_f}\left(1-\frac{{r_s}^2}{{r_p}^2}\right)\frac{dz_f}{dt}}{\frac{\gamma-1}{\gamma}+\frac{1}{\gamma}\frac{{r_s}^2}{{r_p}^2}} \quad \ldots\ldots 2.7$$

Which r_p is the radial piston position, r_s is the radial shock front position and z_f is the axial piston position (Figure 2.6).

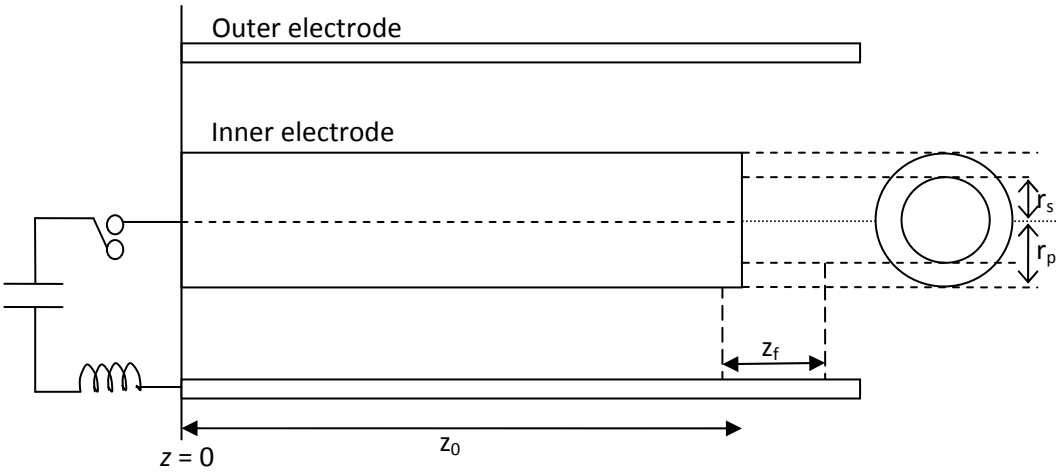

Figure 2.6: The position of the piston and shock front of the plasma slug.

In consideration that the system now consists of the full inductance of the axial phase and the inductance in the radial direction (due to the pinching effect), an equivalent circuit that is similar to that condition is illustrated as below (Figure 2.7):

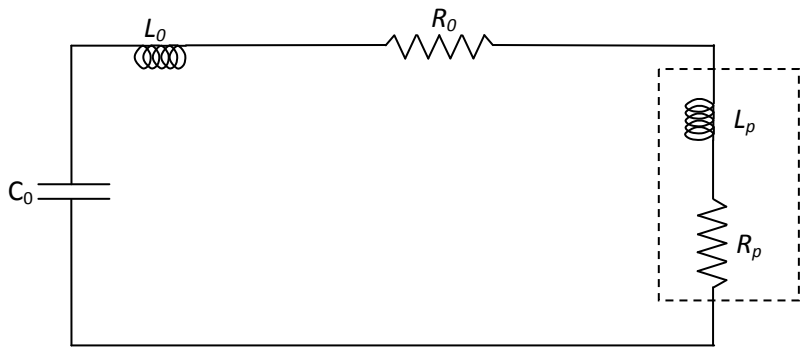

Figure 2.7: The equivalent circuit corresponding to the radial phase.

$$\frac{d}{dt}\left[(L_0 + L_p)I\right] + I(R_0 + R_p) = V_0 - \frac{\int_0^t Idt}{C_0}$$

Since

$$\frac{d}{dt}\left[(L_0 + L_p)I\right] \gg I(R_o + R_p)$$

Thus,

$$L = \frac{\mu_0}{2\pi}(\ln c)z_0 + \frac{\mu_0}{2\pi}\left(\ln\frac{b}{r_p}\right)z_f$$

where z_f and r_p vary with time.

Therefore, the circuit equation is

$$\left\{L_0 + f_c\frac{\mu}{2\pi}(\ln c)z_0 + f_c\frac{\mu}{2\pi}\left(\ln\frac{b}{r_p}\right)z_f\right\}\frac{dI}{dt} + f_c I\frac{\mu}{2\pi}\left(\ln\frac{b}{r_p}\right)\frac{dz_f}{dt} - f_c I\frac{\mu}{2\pi}\frac{z_f}{r_p}\frac{dr_p}{dt} + r_0 I$$
$$= V_0 - \frac{\int Idt}{C_0}$$

Giving the rate of change of current as

$$\frac{dI}{dt} = \frac{V_0 - \frac{\int Idt}{C_0} - r_0 I - f_c\frac{\mu}{2\pi}\left(\ln\frac{b}{r_p}\right)I\frac{dz_f}{dt} + f_c\frac{\mu}{2\pi}\frac{z_f}{r_p}I\frac{dr_p}{dt}}{L_0 + f_c\frac{\mu}{2\pi}(\ln c)z_0 + f_c\frac{\mu}{2\pi}\left(\ln\frac{b}{r_p}\right)z_f} \quad \ldots\ldots(2.8)$$

Equations (2.5), (2.6), (2.7) and (2.8) can be normalized and integrated to give r_s, r_p, z_f and I.